Serum differential proteomics analysis between papillary thyroid cancer patients with ^{131}I-avid and those with non-^{131}I-avid lung metastases

Yan-Hong Xu[1,2] MD,
Wen-Jing Wang[3] MD,
Hong-Jun Song[2] MD,
Zhong-Ling Qiu[2] MD,
Quan-Yong Luo[2] MD

1. Postgraduate Department, Shanghai Jiao Tong University, Shanghai 200025, China
2. Department of Nuclear Medicine, Shanghai Sixth People's Hospital, Shanghai Jiao Tong University, Shanghai 200233, China
3. Department of Molecular Biology for Public Health, Shanghai Municipal Center for Disease Control and Prevention, Shanghai 200336, China.

***

Keywords:
Papillary thyroid carcinoma
- Mass spectrometry
- Proteomics
- Lung metastasis
- Iodine-131 uptake

Correspondence address:
Quan-Yong Luo, Department of Nuclear Medicine, Shanghai Sixth People's Hospital, Shanghai Jiao Tong University, 600 Yishan Rd., Shanghai, 200233, China.
Tel: 86-21-64369181,
Fax: 86-21-64701361
E-mail: lqyn@sh163.net

Received:
12 August 2011
Accepted revised:
23 August 2011

Abstract

Our aim was to compare the differences in serum protein fingerprints between papillary thyroid carcinoma (PTC) patients with ^{131}I–avid lung metastases and those with non-^{131}I-avid lung metastases, and to establish a screening model for screening ^{131}I uptake in lung metastases. *We collected* serum samples from 46 PTC patients with ^{131}I-avid lung metastases (Group A) and 23 PTC patients with non-^{131}I-avid lung metastases (Group B) respectively, and both groups were matched for age and sex, without history of other tumors. Among them, 28 cases (19 cases in Group A, and 9 cases in Group B) were enrolled in the training set to establish the decision tree model, and another 41 cases (27 cases in Group A, and 14 cases in Group B) were incorporated for blind test set. The serum protein fingerprints were profiled using surface enhanced laser desorption/ionization time-of-flight mass spectrometry (SELDI-TOF-MS, USA) and the difference between the two groups was compared using the Ciphergen Proteinchip 3.1 software. Bioinformatics analysis was performed to construct the decision tree model based on the data of the training set, and the blind test was also conducted for blind test set. *Our results* showed that a total of 151 valid protein peaks were detected at the molecular range of 1300Da to 15000Da, among which 7 were significantly different between Group A and Group B ($P < 0.05$). The blind test was conducted via the decision tree model, with a sensitivity of 92.6% (25/27) and a specificity of 85.7% (12/14). *In conclusion*, the difference in the serum protein fingerprints between Group A and Group B is quite accurate for screenning ^{131}I uptake in the lung metastases from PTC, conferring important clinical value for the prediction of ^{131}I uptake and guiding of personalized ^{131}I treatment decisions.

Hell J Nucl Med 2011; 14(3): 228-233 *Published on line: 10 November 2011*

Introduction

Papillary thyroid carcinoma (PTC) accounts for the majority of differentiated thyroid carcinoma (DTC), as the most common thyroid cancer. The most common site of distant metastasis is the lung [1]. If early diagnosis and effective treatments are unavailable, the 5-year death rate remains as high as 70% [2]. Iodine-131 (^{131}I) treatment is the preferred treatment approach for DTC metastases, and the significant uptake of ^{131}I in metastases is a prerequisite for achieving favorable therapeutic effects. Nevertheless, in clinical practice, approximately 10%-20% of patients with DTC lung metastases exhibit non-^{131}I-uptake, which makes those patients unsuitable for ^{131}I treatment. As we know, the routine clinical method of predicting the ability of ^{131}I uptake in metastases is the diagnostic ^{131}I whole-body scan (^{131}I-WBS), however, which is only applicable by thyroxin withdrawal. Therefore, we would prefer to explore a simple serum approach to screen the ability of ^{131}I uptake in lung metastases in DTC patients.

The serum proteome reflects all proteins and peptides that may be related with one gene and allows a more detailed evaluation of disease status using the human proteome. In this study, differential proteomic analysis on PTC patients with and without ^{131}I uptake in lung metastases was performed to scan differentially expressed serum protein fingerprints between both groups. At present, the mechanism of the non-^{131}I-avid lung metastases from PTC is not well understood. Serum proteomics may be a research tool for assisting to understand the mechanism of patients with non-^{131}I-avid lung metastases.

At the same time, if proteomics is adopted to identify serum protein fingerprints differences to screen the ability of ^{131}I uptake in lung metastases of DTC, the ^{131}I uptake can be predicted in advance consequently, and those patients with significant ^{131}I uptake can be chosen to receive ^{131}I treatment. In turn, for those patients with non-^{131}I-uptake, ineffective ^{131}I treatment can be avoided, which is undoubtedly valuable for improving the therapeutic efficacy and reducing toxicity. Thus, one could have an alternative method to predict the ability of metastatic ^{131}I uptake before ^{131}I treatment in addition to the diagnostic ^{131}I-WBS.

Materials and methods

General information

Specimen sources

To implement the ^{131}I treatment, thyroxin withdrawal for at 3 weeks was required before blood samples were drawn and ^{131}I administered. Patients were instructed to avoid food containing iodine for 2 weeks. Serum thyroid stimulating hormone (TSH), thyroglobulin (Tg) and Tg antibody (TgAb) were measured in all patients before ^{131}I treatment. Serum samples of 69 PTC patients with (Group A) and without (Group B) ^{131}I uptake in lung metastases were collected. Both groups were matched for age and gender, without history of other tumors. The criteria for lung metastases is bilateral diffuse pulmonary nodules confirmed by CT scan combined with increased serum Tg level and could not be due to other causes like inflammatory or cancerogenic disease. After the ablation of residual thyroid gland, ^{131}I-WBS showed diffuse uptake of ^{131}I in the lung were enrolled in Group A. In turn, ^{131}I-WBS showed no ^{131}I uptake in lung metastases were enrolled in Group B. The clinical features of the two groups were summarized in Table 1.

Grouping

The patients were divided into training set and blind test set, among which 28 cases incorporated in training set (19 cases in Group A, and 9 cases in Group B) were utilized to establish decision tree model, and another 41 cases enrolled in blind test set (27 cases in Group A, and 14 cases in Group B) were set for blind test.

Chips and reagents

Sodium acetate (NaAc), acetonitrile, trifluoroacetic acid (TFA), sinapinic acid (SPA) were purchased from Sigma (St. Louis, MO, USA), immobilized metal affinity capture chips (IMAC3) and protein chip reader (PBS-IIc), Ciphergen Proteinchip 3.1 were purchased from Ciphergen Biosystems Inc (Fremont, CA, USA).

Serum sample preparation

Peripheral blood serum samples from patients in Group A and Group B were respectively collected under identical conditions of specimen collection, serum separation and specimen storage. After staying at room temperature for 2h, samples were centrifuged at 3000r/min for 15min, and supernatants were collected, aliquoted in 20μL portions and frozen at -80°C for future use. The frozen aliquots of serum sample were taken out and thawed on ice, and afterwards they were centrifuged for 10min at 12000r/min at 4°C to exclude the insoluble substances. The chips were activated by adding 100mmol/L $CuSO_4$ (10μL per well) and shaken in wet box, twice for 10min each. After $CuSO_4$ was removed, it was followed by three de-ionized (DI) water rinses. 10μL of 50mmol/L NaAc (pH 4.0) was added and stirred for 2min in wet box. It was washed three times in DI water after removal of NaAc. The ProteinChip Assay Cassette was placed in the Bioprocessor, and washed twice at room temperature for 5min with 200μL binding buffer (PBS with 500mmol/L NaCl, pH 7.2, 200μL per well) to balance chips.

Of each sera sample 6μL was diluted in 234μL PBS containing 500mmol/L NaCl (pH7.2), added to each well (200μL per well), and incubated for 90min at room temperature on an orbital shaker with shaking at 900rpm. The ProteinChip arrays were then eluted 2 times using PBS containing 500mmol/L NaCl (pH 7.2, 200μL per well), and the ProteinChip arrays were washed using 300μL deionized water. Each 0.5μl of saturated solution of SPA in 50% acetonitrile and 0.15% TFA was applied to each spot. After air drying, another 0.5μL of SPA was added to each spot.

Table 1. *Clinical features of Group A and Group B in this study*

Clinical features		Group A	Group B
Total		46	23
Mean age (years)		48.73±5.46	49.92±6.24
Gender (male/female)		15/31	7/16
Histologic variants of PTC		1 follicular variant of PTC	1 follicular variant of PTC
Duration of disease (months)		6.31±2.04	6.58±2.93
Stage of PTC	I	14	7
	IV	32	16
Prior radioiodine treatment		0	0
Method of TSH elevation		Thyroxin withdrawal for 3 weeks	Thyroxin withdrawal for 3 weeks
Results of CT scan of lung		Diffuse small nodules	Diffuse small nodules
Serum Tg level (ng/ml)		1896.45±53.07	1678.87±39.45
Serum TgAb level (IU/ml)		193.64±19.28	206.23±20.14
^{131}I-WBS results		Diffuse ^{131}I uptake in the lung	No ^{131}I uptake in the lung
Extent of disease		no other distant metastasis	no other distant metastasis

Data acquisition

All ProteinChip Arrays were read on a ProteinChip reader (PBS-IIc). The parameters of the ProteinChip reader were set as follows. Time-of-flight (TOF) spectra had an intensity of 165 arbitrary units and a detector sensitivity of 7 with an optimum range of 1000-10000Da, and maximal molecular weight of 30000Da.

Peaks were detected automatically using Ciphergen ProteinChip Software Version 3.1 and polar plot was drawn, where the vertical axis represented the relative content of protein and the abscissa axis represented the mass-to-charge ratio (M/Z). All mappings were calibrated according to the total ion current to reduce the experimental errors caused by factors like chips differences and fluctuation of apparatus. The differences between peaks of proteins with identical mass-charge ratio in Groups A and B were assessed as P value, which was calculated by the Ciphergen Proteinchip 3.1 software. Valid protein peaks were defined as those with signal to noise ratios (S/N) greater than 5 and with the minimum peak threshold (% of all spectra) greater than 10%.

Establishment of decision tree and blind test

The data from the training set was used to calculate to build up the decision tree model. After 500-time cross validations were ran and the model that had the highest predictive accuracy was selected for optimal decision tree model and in turn the samples in blind test set were classified based on this model. The predictive method was as follows: For a sample from blind test set, if the predictive results turned out to prove it in Group A and really it came from Group A, a right result was achieved; on the contrary, the result was wrong. If the predictive results turned out to prove it in Group B and really it came from Group B, a right result was achieved; on the contrary, the result was wrong.

Statistical analysis

The differences in expression of protein with same M/Z between Groups A and B were statistically analyzed by the Wilcoxon rank-sum test.

Results

Differentially expressed proteins between Group A and Group B

One hundred and fifty-one peaks were detected within a molecular weight range of 1300-15000Da, and seven of them yield statistically significant differences (P<0.05). Among the seven peaks, five displayed high expression in the Group A, and two peaks showed high expression in Group B, as shown in Table 2. The box plot displaying the differential proteins peaks between Group A and Group B is shown in Figure 1 and the protein mass spectrometry of one protein peak exhibiting high expression in Group B is shown in Figure 2.

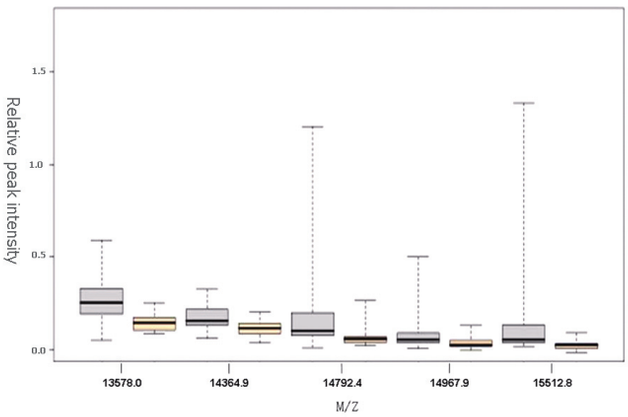

Figure 1. The comparison between box plots of protein peaks in Group A and Group B. The peaks at M/Z 13578.0Da, 14364.9Da, 14792.4Da, 14967.9Da and 15512.8Da, displayed high expression in the Group A. (The peaks at M/Z 3889.8Da and 4193.8Da which showed high expression in Group B are not incorporated in this figure due to over-expression)

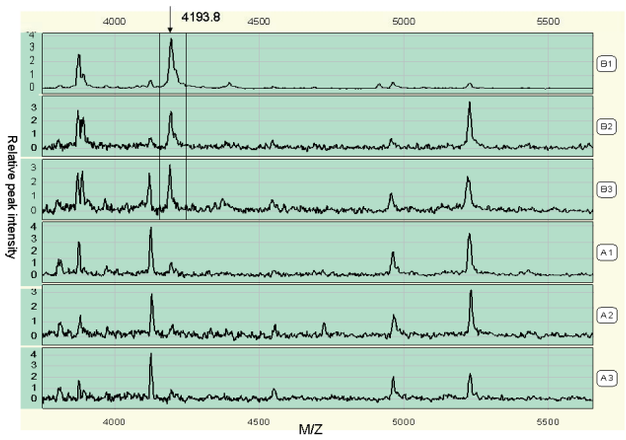

Figure 2. The protein fingerprints of differential protein peaks at M/Z of 4193.8Da in Group A and Group B (A1-A3 represent serum protein fingerprints in Group A and the peak at M/Z of 4193.8Da exhibited low protein expression; B1-B3 represent serum protein fingerprints in Group B and the peak at M/Z of 4193.8Da exhibited high protein expression).

Establishment of decision tree and blind test

An unsupervised cluster analysis was applied to the differential proteins peaks, and the relationship between Group A and Group B in training set is shown in Figure 3. The training sets underwent 500-time cross validations, and then the decision tree producing the highest accuracy

Table 2. *Differentially expressed protein peaks between Group A and Group B*

Index	M/Z (Da)	Relative Peak Intensity		P
		Group A	Group B	
1	3889.8	1.95±2.27	3.87±3.12	0.0106
2	4193.8	3.54±5.49	6.21±9.16	0.0319
3	13578.0	0.27±0.12	0.15±0.05	0.0001
4	14364.9	0.18±0.07	0.12±0.05	0.0062
5	14792.4	1.02±2.98	0.07±0.06	0.0029
6	14967.9	0.42±1.21	0.04±0.04	0.0237
7	15512.8	0.66±2.00	0.02±0.03	0.000058

after cross validations was chosen as optimal decision tree model, in which 3 layers and 4 nodes are included (Fig. 4). The optimal decision tree was used to perform classification and screening for 41 samples in blind test set. As a result, 37cases were accurately judged with a correct classification rate of 90.2% (37/41), a sensitivity of 92.6% (25/27) and a specificity of 85.7% (12/14).

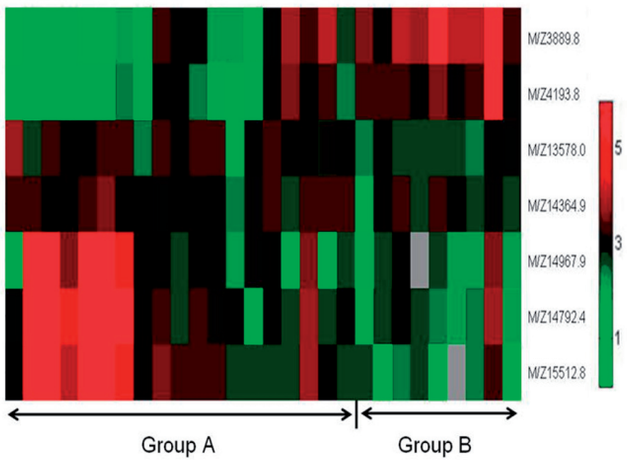

Figure 3. Cluster analysis conducted for significant differences in protein peaks between Group A and Group B in the training set (each line represents one protein, each column represents a serum sample , red represents higher level of serum proteins, and green represents lower levels of serum proteins)

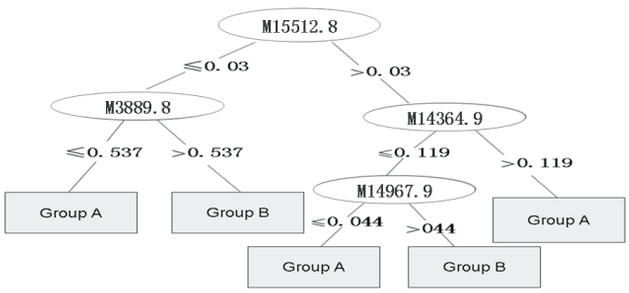

Figure 4. The optimal decision tree model for screening the ^{131}I uptake in lung metastases from PTC. The relative peak intensity of differentially expressed protein (M/Z=15512.8Da) was≤0.03, and the relative peak intensity of protein (M/Z=3889.8Da) was≤0.537 was considered from Group A; The relative peak intensity of protein (M/Z=15512.8Da) was≤0.03, and the relative peak intensity of protein (M/Z=3889.8Da) was>0.537 was considered from Group B; The relative peak intensity of protein (M/Z=15512.8Da) was>0.03, and the relative peak intensity of protein (M/Z=14364.9Da) was>0.119 was considered from Group A; The relative peak intensity of protein (M/Z=15512.8Da) was>0.03, the relative peak intensity of protein (M/Z=14364.9Da) was≤0.119, and the relative peak intensity of protein (M/Z=14967.9Da) was≤0.044 was considered from Group A; The relative peak intensity of protein (M/Z=15512.8Da) was>0.03, the relative peak intensity of protein (M/Z=14364.9Da) was≤0.119, and the relative peak intensity of protein (M/Z=14967.9Da) was>0.044 was considered from Group B) .

Discussion

Postoperative ^{131}I treatment is preferred as the first-line treatment for DTC patients [3]. Sixty years of clinical practice has confirmed that ^{131}I treatment is effective in reducing postoperative recurrence and metastases of DTC. It plays dual roles in diagnosis and treatment of DTC, which can greatly improve patients' quality of life and prolong their survival. The prerequisite for accomplishing favorable ^{131}I treatment is the metastases are ^{131}I-avid, so the β-ray released during ^{131}I decay can directly kill tumor cells, delivering a strong therapeutic effect.

The lung is the most common site for distant metastases from DTC and most of the DTC lung metastases are ^{131}I-avid, so plausible therapeutic effect can be achieved by ^{131}I treatment. Nevertheless, there are still 10%-20% of DTC patients who have no uptake of ^{131}I in lung metastases in the clinic practice, are irresponsive to ^{131}I treatment and cannot be treated with ^{131}I. Currently, large doses of ^{131}I are generally given for one or two times postoperatively, and ^{131}I-WBS is performed to assess the capacity of ^{131}I uptake in the lung metastases. If the lung metastases are detected to be ^{131}I-avid, patients will continue to receive ^{131}I treatment; on the other hand, if lung metastases show low or no ^{131}I uptake, patients have obviously been subjected to unnecessary ^{131}I treatment and risks of radiation incurred by ^{131}I and unnecessary stopping taking thyroid hormone before treatment.

If the ^{131}I uptake in DTC metastases can be predicted in advance, on which a reasonable treatment plan can be developed before treatment, it will undoubtedly help to improve the clinical remission rate and long-term survival rates for patients. The diagnostic ^{131}I-WBS could predict the ability of metastatic ^{131}I uptake before ^{131}I treatment. However, the mechanism of the non-^{131}I-avid lung metastases from PTC is not well understood. Even though researches believe [4] that fluoro-18-fluorine-desoxy-glucose positron emission tomography (^{18}F-FDG-PET) scan is of clinical value in determining the degree of malignancy, they hold that high ^{18}F-FDG uptake presenting in the metastatic tumors indicates a relatively low degree of tumor differentiation and a relatively high level of malignancy, which leads to loss of ^{131}I uptake, that is, ^{131}I uptake is negatively correlated with ^{18}F-FDG uptake (flip-flop phenomenon). However, for some DTC patients with distant metastases, the uptake of ^{18}F-FDG and ^{131}I can occur simultaneously, which pose a hurdle in prediction. In addition, ^{18}F-FDG-PET examination is expensive, which is unaffordable for part of the patients. Therefore, exploring an affordable, easy and effective way to screen the ^{131}I uptake in DTC metastases is well needed.

Since PTC accounts for the vast majority of DTC, the PTC patients with lung metastases were enrolled as subjects in this research. We sought to identify the serum proteins that associated with ^{131}I uptake in lung metastases via serum differential proteomics analyses, so the ^{131}I uptake could be screened based on the results, besides the diagnostic ^{131}I-WBS.

Multiple genes are involved during the occurrence and development of diseases, which can induce changes of a large variety of proteins [5]. The changes in quality and quantity of serum proteins presenting at early stage of disease, can be measured through proteomics approaches and the biomarkers related to the earliest signs of disease can be screened [6]. Proteomics technology is used as a screening test for different proteins expressed in various stages of cancers, especially for tumor-associated low abundance serum proteins, which can accurately monitor the changes in protein spectrum during diseases [7]. The SELDI-TOF-MS applied in this study integrates protein chip technology with mass spectrometry and incorporates sam-

ple separation and purification with biochemical reactions and detection. It is characterized by advantages of low-cost (15~20$ per test), high-speed analysis, small amount of sample, high specificity and resolution, and high throughput with high selectivity, and is widely utilized for the detection and screening of various disease-specific biomarkers and for determination of small molecules in serum as well as the development of new drugs [8, 9]. A series of new markers with high sensitivity and specificity used for early diagnosis of malignant tumors, including head and neck cancer [9], bladder cancer [10], prostate cancer [11-14], ovarian cancer [15, 16], breast cancer [17-18], liver cancer [19] and lung cancer [20, 21], have been identified by this methodology. In the view of the proteomics analysis in DTC, Wang et al. (2010) [22] adopted weak cation exchange (WCX2) chip to detect the protein fingerprints of PTC, benign thyroid nodes and normal serum, finding that there was significantly difference in serum proteomic patterns between different pathological types and stages of thyroid cancers. The serum protein fingerprints of PTC patients and normal people were detected by Fan et al. (2009) [23] using WCX2 chip, and a diagnostic model for PTC was established based on serum protein fingerprints.

In the present study, the differentially serum proteins in PTC patients with ^{131}I–avid lung metastases and those with non-^{131}I-avid lung metastases were identified for the first time using IMAC3 chip based SELDI-TOF-MS, and corresponding screening models was established to effectively screen the ^{131}I uptake of lung metastases from PTC. The results show that 7 protein peaks had significant difference in expression between both groups ($P<0.05$), and their M/Z were 3889.8Da, 4193.8Da, 13578.0Da, 14364.9Da, 14792.4Da, 14967.9Da and 15512.8Da, respectively. Five of the seven proteins displayed high expression in Group A, and two (M/Z=3889.8Da and M/Z=4193.8Da) demonstrated high expression in Group B. No study reported in the literature indicated that other lung metastases coming from other primary cancers, or other lung diseases, including inflammatory or primary lung cancer show the same proteomics characteristics as of lung metastases from PTC reported here by us. The decision tree built in this study exhibits high accuracy in classifying and screening the ^{131}I uptake in lung metastases from PTC, and it had an accuracy rate of 90.2%, a sensitivity of 92.6% and specificity of 85.7%.

In conclusion, in the present original study, serum differential proteomics analysis was applied based on the SELDI-TOF-MS, which can detect the significant discrepancy in serum protein fingerprints between PTC patients with ^{131}I-avid lung metastases and those with non-^{131}I-uptake lung metastases. This difference can successfully screen the ability of ^{131}I uptake of lung metastases which is valuable for clinical decision making and personalized ^{131}I treatment planning and thus has high application potential. Further, mass spectrometry is deserved to be used as a research tool for assisting our understanding the iodine transport and secretary and metabolic properties of DTC patients with non- ^{131}I-uptake metastases.

Acknowledgements

We thank Dr Hua-Zong Zeng from Shanghai Minxin Information Technology Co., Ltd, who provided strong data analysis support for this study.

This research was supported by the New One Hundred Person Project of the Shanghai Jiao Tong University Medical School. The authors have nothing to declare for the other relevant categories.

There is no conflict of interest that could be perceived as prejudicing the impartiality of the research reported.

Bibliography

1. Schlumberger MJ. Papillary and follicular thyroid carcinoma. *N Engl J Med* 1998; 338: 297-306.
2. Ronga G, Filesi M, Montesano T et al. Lung metastases from differentiated thyroid carcinoma. A 40 years' experience. *Q J Nucl Med Mol Imaging* 2004; 48: 12-9.
3. Woodrum DT, Gauger PG.. Role of ^{131}I treatment of well differentiated thyroid cancer. *J Surg Oncol* 2005; 89: 114-2l.
4. Kim WG, Ryu JS, Kim EY et al. Empiric high-dose 131-iodine treatment lacks efficacy for treated papillary thyroid cancer patients with detectable serum thyroglobulin, but negative cervical sonography and ^{18}F-fluorodeoxyglucose positron emission tomography scan. *J Clin Endocrinol Metab* 2010; 95: 1169-73.
5. Huang YJ, Xuan C, Zhang BB et al. SELDI-TOF MS profiling of serum for detection of nasopharyngeal carcinoma. *J Exp Clin Canc Res* 2009; 28: 85.
6. Weinberger SR, Moris TS, Pawiak M. Recent trends in protein biochip technology. *Pharmacogenomics* 2000; l: 395-416.
7. Cravatt BF, Simon GM, Yates JR 3rd. The biological impact of mass-spectrometry-based proteomics. *Nature* 2007; 450: 991-1000.
8. Li G, Zhang W, Zeng H et al. An integrative multi-platform analysis for discovering biomarkers of osteosarcoma. *BMC Cancer* 2009; 9: 150.
9. Wadsworth JT, Somers KD, Cazares LH et al. Serum protein profiles to identify head and neck cancer. *Clin Cancer Res* 2004; 10: 1625-32.
10. Vlahou A, Schellhammer PF, Mendrinos S et al. Development of a novel proteomic approach for the detection of transitional cell carcinoma of the bladder in urine. *Am J Pathol* 2001; 58: 1491-501.
11. Adam BL, Qu Y, Davis JW et al. Serum protein fingerprinting coupled with a pattern-matching algorithm distinguishes prostate cancer from benign prostate hyperplasia and healthy men. *Cancer Res* 2002; 62: 3609-14.
12. Qu Y, Adam BL, Yasui Y et al. Boosted decision tree analysis of surface-enhanced laser desorption/ionization mass spectral serum profiles discriminates prostate cancer from noncancer patients. *Clin Chem* 2002; 48: 1835-43.
13. Wagner M, Naik DN, Pothen A et al. Computational protein biomarker prediction: a case study for prostate cancer. *BMC Bioinformatics* 2004; 5: 26.
14. Jr GW, Cazares LH, Leung SM et al. Proteinchip surface enhanced laser desorption/ionization (SELDI) mass spectrometry: a novel protein biochip technology for detection of prostate cancer biomarkers in complex protein mixtures. *Prostate Cancer Prostatic Dis* 1999; 2: 264-76.
15. Petricoin EF, Ardekani AM, Hitt BA et al. Use of proteomic patterns in serum to identify ovarian cancer. *Lancet* 2002; 359: 572-7.
16. Vlahou A, Schorge JO, Gregory BW et al. Diagnosis of ovarian cancer using decision tree classification of mass spectral data. *J Biomed Biotechnol* 2003; 5: 308-14.

17. Li J, Zhang Z, Rosenzweig J et al. Proteomics and bioinformatics approachs for identification of serum biomarkers to detect breast cancer. *Clin Chem* 2002; 48: 1296-304.
18. Vlahou A, Laronga C, Wilson L et al. A novel approach toward development of a rapid blood test for breast cancer. *Clin Breast Cancer* 2003; 4: 203-9.
19. Poon TC, Yip TT, Chan AT et al. Comprehensive proteomic profiling identifies serum proteomic signatures for detection of hepatocellular carcinoma and its subtypes. *Clin Chem* 2003; 49: 752-60.
20. Xiao X, Liu D, Tang Y et al. Development of proteomic patterns for detecting lung cancer. *Dis Markers* 2003; 19: 33-9.
21. Zhukov TA, Johanson RA, Cantor AB et al. Discovery of distinct protein profiles specific for lung tumors and pre-malignant lung lesions by SELDI mass spectrometry. *Lung Cancer* 2003; 40: 267-79.
22. Wang JX, Yu JK, Wang L et al. Application of serum protein fingerprints in diagnosis of papillary thyroid carcinoma. *Proteomics* 2006; 6: 5344-9.
23. Fan Y, Shi L, Liu Q et al. Discovery and identification of potential biomarkers of papillary thyroid carcinoma. *Mol Cancer* 2009; 8: 79.

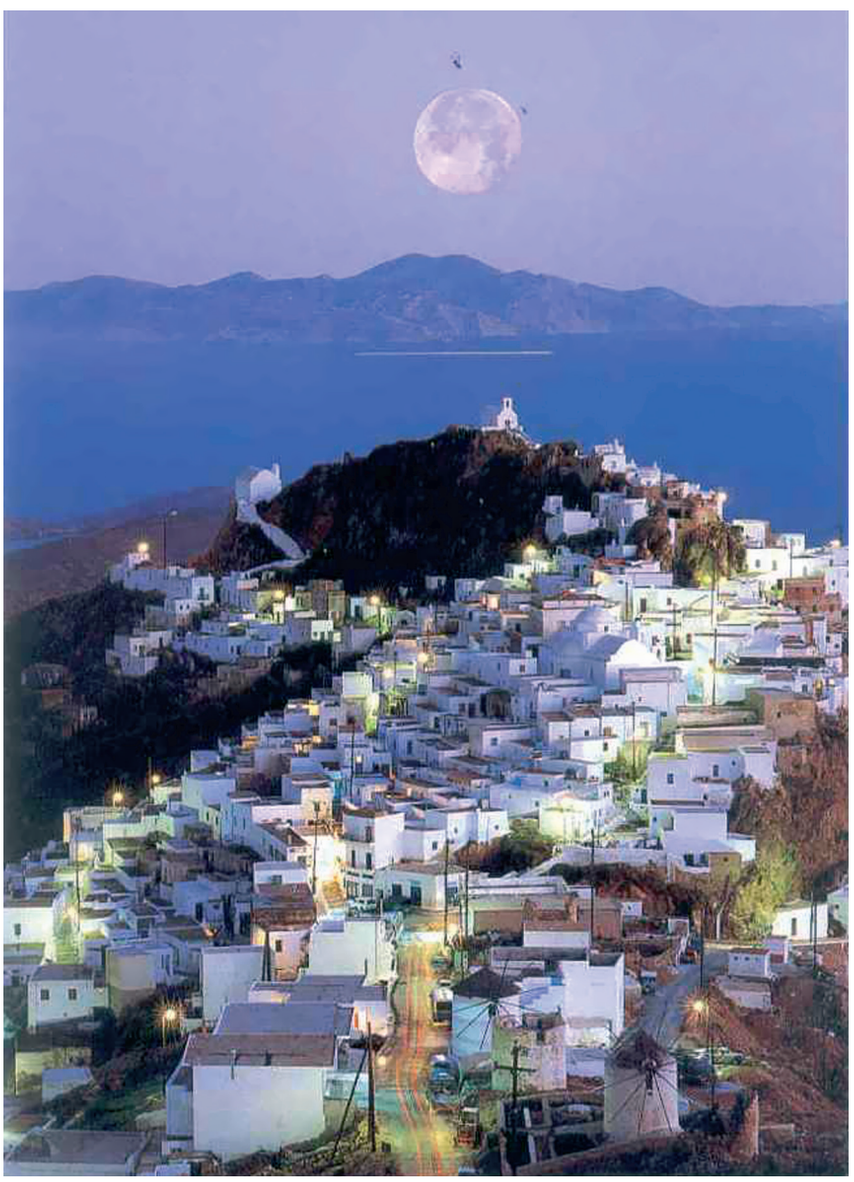

Sunset from Serifos, a Cycladic island in the Aegean Sea, Greece.